

Supplemental Materials

Molecular Biology of the Cell

Cao et al.

Supplemental Figure Legends

Figure S1. Domain structure of three *Dictyostelium* arrestin homologs. (A) Analysis of the *D. discoideum* genome sequence revealed three arrestin homologs containing both Arrestin-N and Arrestin-C domains, named AdcA-C. In addition to Arrestin-N and Arrestin-C domains present in all three homologs, other motifs identified include: C2 domain (phospholipid binding site), SAM protein interaction module (for homo- and hetero-oligomerization with other SAM domains), TM (putative transmembrane domain), and FYVE (phosphatidylinositol 3-phosphate binding domain). The % similarities of the Arrestin –N and Arrestin-C domains of the three *Dictyostelium* arrestins are shown. (B) Protein alignment between AdcB and AdcC were performed using software of ClustalX1.83.

Figure S2. Generation of arrestin null cells. (A) Disruption of arrestin genes was achieved by homologous recombination using a selectable Blasticidin resistance (BSR) marker. (B) The double disruption of *adcB* and *adcC* was accomplished using the Cre-LoxP system. Following the first disruption, Blasticidin sensitivity was restored by introducing Cre recombinase to excise the LoxP-flanked BSR cassette, leaving stop codons in the disrupted gene. By recycling the selectable marker in this manner, *adcB⁻C⁻* cell line was generated. (C) PCR screening with primers flanking each gene demonstrates the expected ~1.3 kb size increase of PCR products in null cells.

Figure S3. Development of arrestin null cells on bacterial lawns. Wild-type, *adcB⁻*, *adcC⁻*, *adcB⁻C⁻* and *adcB⁻C⁻* cells expressing AdcB -YFP or AdcC -YFP were grown in association with *Klebsiella aerogenes* at 22 °C. Photographs were taken after 5 days.

Figure S4. AdcB does not translocate to plasma membrane upon cAMP stimulation. (A) *adcB⁻* cells expressing AdcB-YFP were stimulated with 10 μM cAMP. Images were captured and frames in the YFP channel at selected time points are shown. The scale bar represents 5 μm. The kinetics of the time course is graphed in (B). Means (n = 5) and SDs are shown.

Figure S5. cAR1 associates with AdcC. (A) Lysates of RI9 cells co-expressing AdcC-mCherry and cAR1-YFP, cm1234-YFP or YFP tag were incubated with beads coupled with anti-GFP antibody for co-IP assays. Elutes were analyzed by immunoblotting using anti-GFP to detect cAR1-YFP, cm1234-YFP or YFP tag (upper panel) and anti-RFP antibody to detect AdcC-mCherry (lower panel) respectively. As control, 5% of the total volumes of the lysates used for the co-IP reactions were also included (input, lane I). (B) Co-IP of cm1234 compared to wild type cAR1 in the absence of cAMP. AdcC-mCherry band of cm1234-YFP (without cAMP stimulation) in Figure 3A was measured by ImageJ and normalized with the level of cAR1-YFP (without cAMP stimulation). Results represent the mean \pm SD of three independent experiments. Statistical significance was assessed by t-test, $P = 0.09$.

Figure S6. Proteins that associate with AdcC. (A) Identification of proteins that associate with AdcC. Cells expressing AdcC-YFP-TAP or YFP-TAP (as a control) were stimulated with 0 or 50 μ M cAMP, suspended in lysis buffer, and then incubated with beads coupled to anti-GFP antibody. After incubation, the beads were washed, and then eluted proteins were subjected to protein gel electrophoresis. Shown is a representative protein gel stained with Coomassie blue. Protein bands were excised for mass spectrometry analysis. (B) A partial list of proteins identified by mass spectrometry that associate with AdcC are shown. (C) AdcC associates with ERK2. Lysates of *adcC*⁻ cells co-expressing RFP-ERK2 and AdcC-YFP or YFP tag (as a control) were incubated with beads coupled with anti-RFP antibody for immunoprecipitation assays. Elutes (lane IP) were subjected to SDS gel electrophoresis and analyzed by immunoblotting using anti-RFP antibody to detect RFP-ERK2 (upper panel) and anti-GFP to detect AdcC-YFP or YFP tag (lower panel) respectively. 5% of the total lysates were reserved to show input levels (lane I).

Figure S7. (A) cAR1 levels are the same in developed wild-type and *adcB*⁻*C*⁻ cells. Lysates of 6-h developed wild-type and *adcB*⁻*C*⁻ cells were subjected to SDS gel electrophoresis and analyzed by immunoblotting using anti-cAR1 antibody. (B) The level of ERK2 is similar in developed wild-type, *adcB*⁻*C*⁻, and *adcB*⁻*C*⁻ expressing AdcC-YFP cells. Cells were developed for 6 hr. The lysates were subjected to SDS gel electrophoresis and the total ERK2 level was analyzed by immunoblotting using

anti-ERK antibody. (C-D) Load control showing the linearity in exposure of anti-pERK2 blots. The peak 1 min time point was loaded as shown in Figures 4B and C and then at $\frac{1}{2}$ and $\frac{1}{4}$ amount of the initial load. Blots were probed and exposed as in Figure 4 and band intensities were quantified and graphed in D with the R^2 value reported.

Figure S8. cAR1-induced ERK2 phosphorylation in *adcB*⁻ and *adcC*⁻ mutant cells. (A-B) The kinetics of ERK2 activation in developed wild-type, *adcB*⁻, and *adcC*⁻ cells in response to a 1 μ M or 50 μ M cAMP stimulation was examined. ERK2 activation was assessed by immunoblotting with anti-phospho-ERK2 (pERK2) antibody. Western blots for actin were used as loading control. The level of pERK2 was normalized to the peak value at 1 min. The kinetics of the time course is graphed in (C-D). Results represent the mean \pm SD of three independent experiments.

Figure S9. cAMP oscillations in arrestin null cells. (A-E) cAMP oscillations were observed in the wild-type, *adcB*⁻, *adcC*⁻, *adcB*⁻*C*⁻, and *adcB*⁻*C*⁻ cells expressing AdcC-YFP during early development by capturing dark field images every 1 min with a stereo microscope. Time plots were generated by measuring intensity changes in the frame-subtracted image sequence. (F) The period of cAMP oscillation was analyzed with 3 mounts per movie and graphed. Means (n = 3) and SDs are shown. Statistical significance was assessed by t-test, **P<0.01. Independent experiments were performed at least twice. (note that the data of wild-type, *adcB*⁻*C*⁻, and *adcB*⁻*C*⁻ cells expressing AdcC-YFP are also shown in Figure 5).

Figure S10. (A-B) Additional examples for data shown in Figure 6A and 6B. Wild-type, *adcB*⁻, *adcC*⁻, and *adcB*⁻*C*⁻ cells expressing cAR1-YFP were stimulated with 50 μ M cAMP. The internalization of cAR1-YFP was imaged using confocal microscopy and photographs were taken before and 1 hr after stimulation. (note that the data of wild-type and *adcB*⁻*C*⁻ cells expressing cAR1-YFP are also shown in Figure 6). (C) Additional examples for data shown in Figure 6C. cAR1-YFP is localized on the post-lysosomes after internalization. Wild-type cells expressing cAR1-YFP were stimulated with 50 μ M

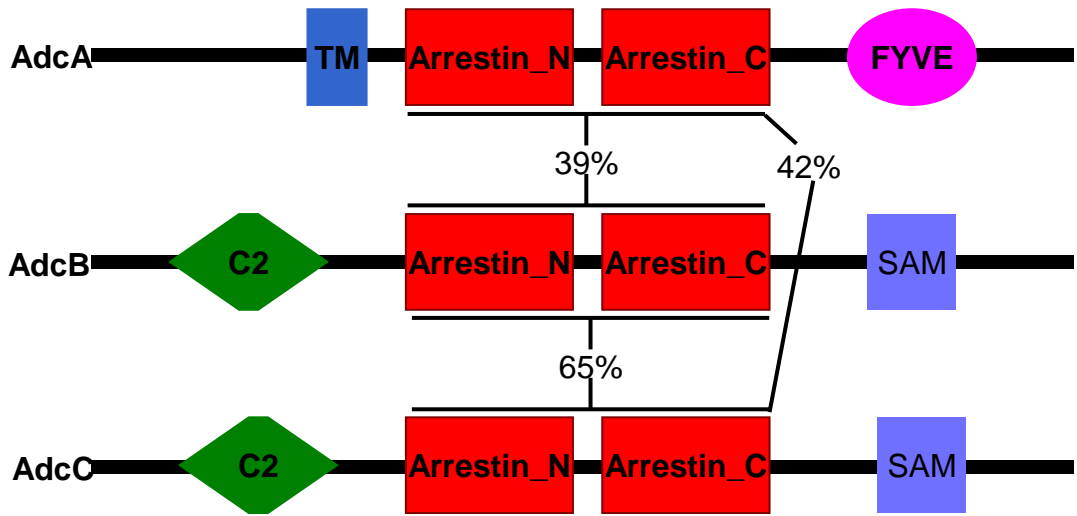
cAMP for 1h, fixed, and processed for immunofluorescence assay with anti-p80. Co-localization of cAR1-YFP and p80 is indicated by arrows. The scale bar represents 5 μm . (D) Additional examples for Figure 6D. cm1234 is defective in internalization. Wild-type cells expressing cm1234-YFP were stimulated with 300 μM cAMP and images were captured at 0 and 2 hr post-stimulation.

Figure S11. (A) cAR1-YFP does not co-localize with p80-positive vesicle in *adcB⁻C⁻* cells. *adcB⁻C⁻* cells expressing cAR1-YFP were stimulated with 50 μM cAMP for 1h, fixed, and processed for immunofluorescence assay with anti-p80. The scale bar represents 5 μm . (B) cAMP-induced AdcC membrane translocation requires Ca^{2+} . *adcC⁻* cells expressing AdcC-YFP in DB buffer were stimulated with 10 μM cAMP. The kinetics of the time course is graphed in (C). Means ($n = 5$) and SDs are shown. (D) *adcC⁻* cells expressing AdcC-YFP that have been incubated in PM buffer (Ca^{2+} free) were stimulated with 10 μM cAMP. The kinetics of the time course is graphed in (E). Means ($n = 5$) and SDs are shown.

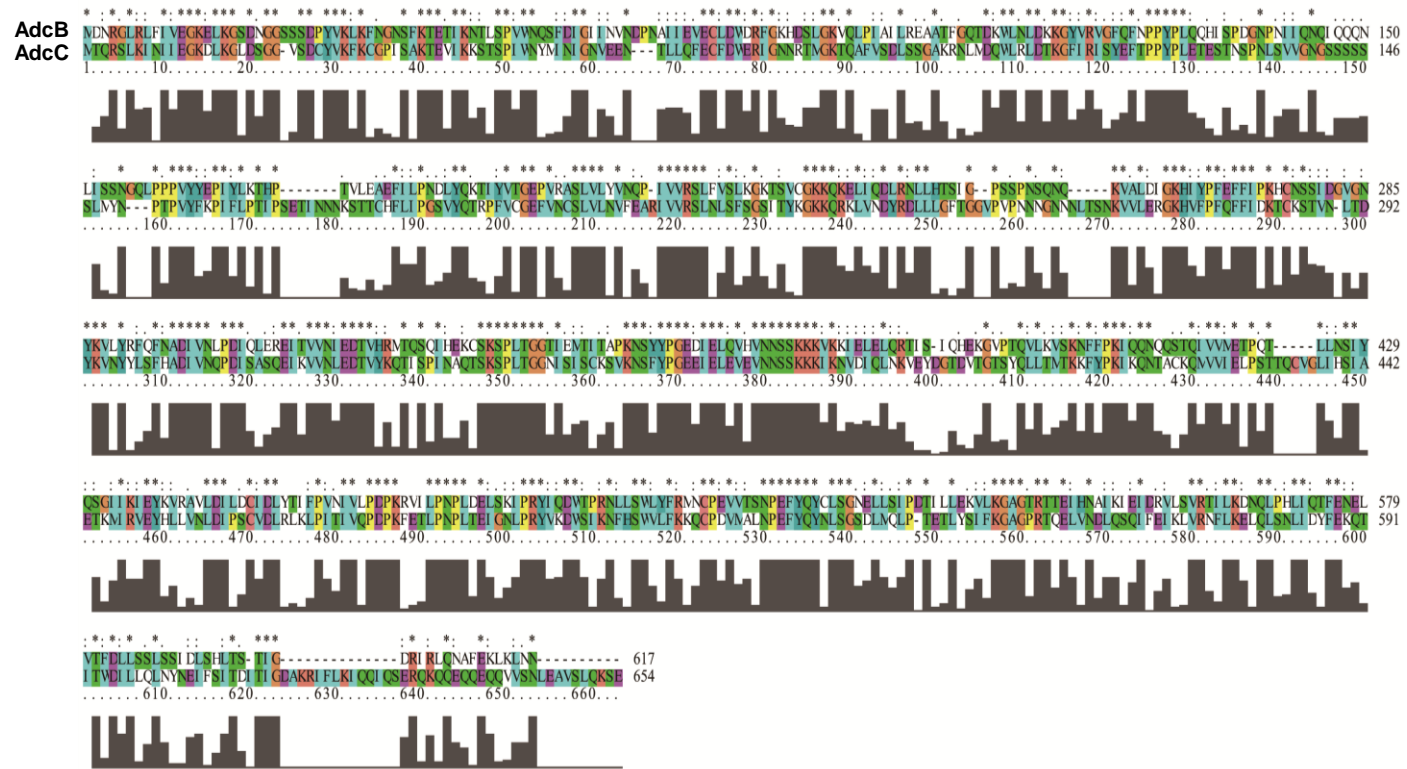
Movie 1. EZ-Taxiscan chemotaxis assay of wild-type cells. Developed wild-type cells are moving in a linear cAMP gradient that ranges from 0-1 μM cAMP. Frames were taken every 15 secs. The source of cAMP is at the bottom of the frame in the movies.

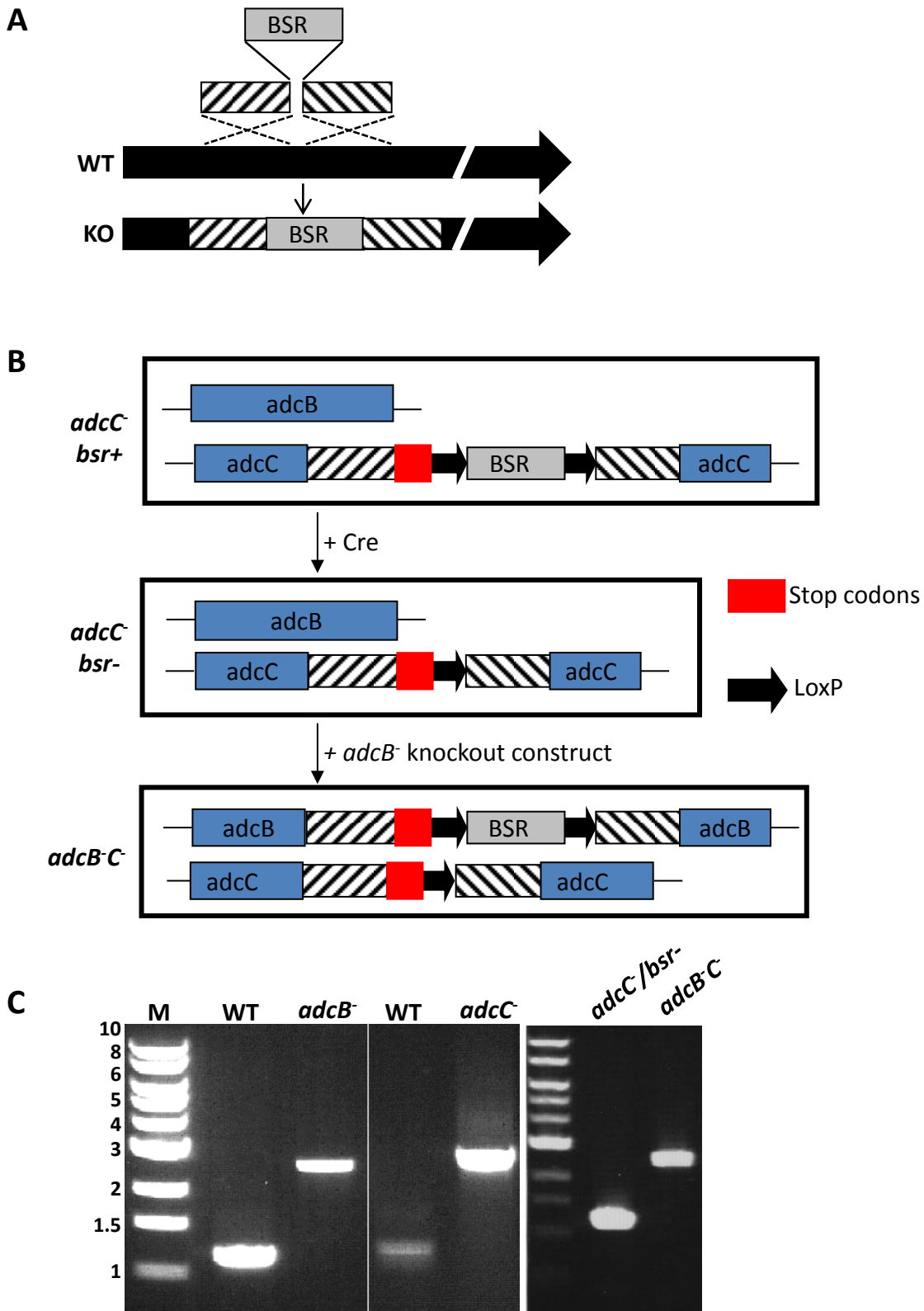
Movie 2. EZ-Taxiscan chemotaxis assay of *adcB⁻C⁻* cells. Developed *adcB⁻C⁻* cells are moving in a linear cAMP gradient that ranges from 0-1 μM cAMP. Frames were taken every 15 secs. The source of cAMP is at the bottom of the frame in the movies.

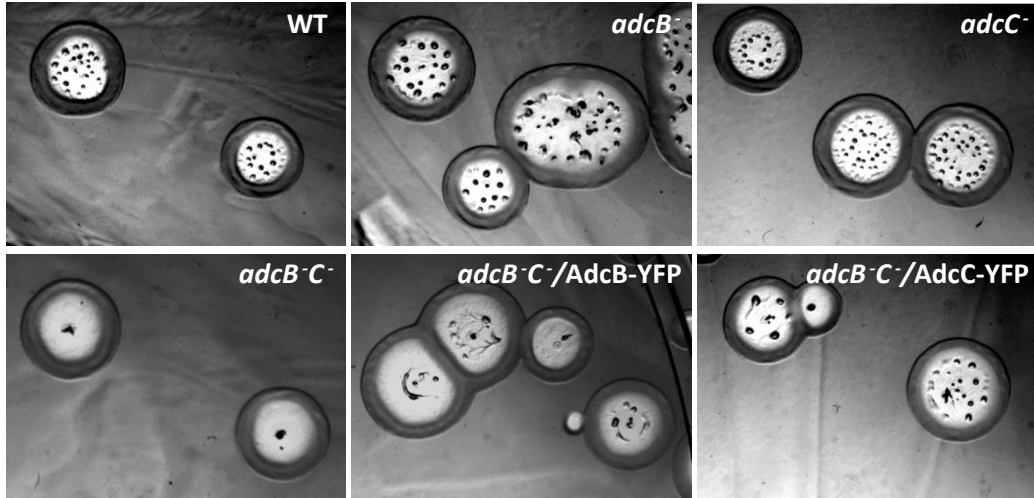
A

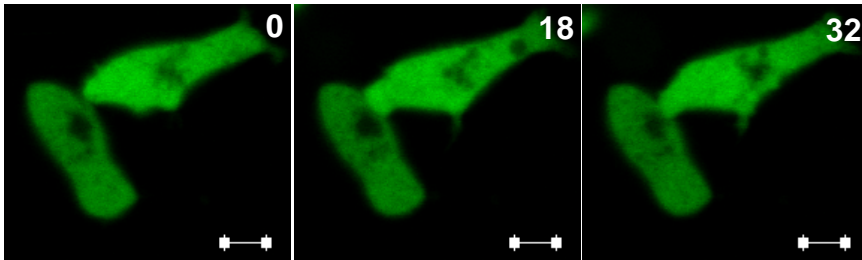
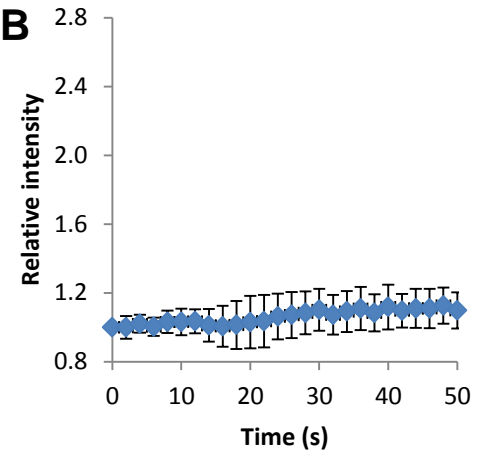


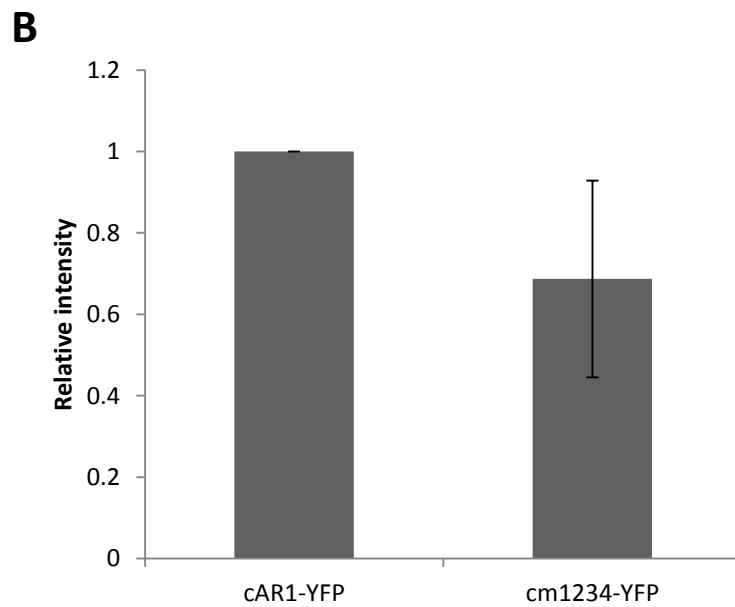
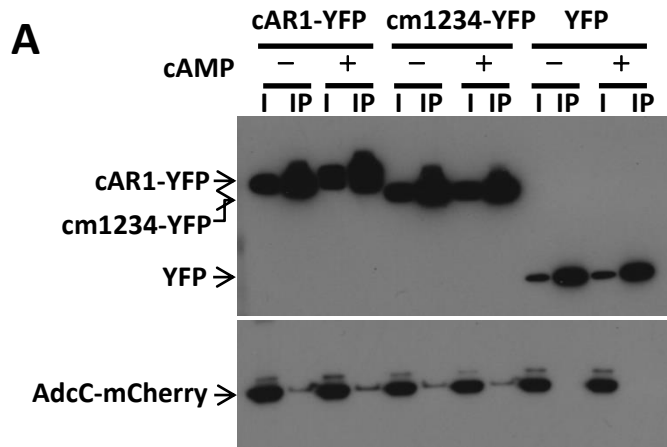
B

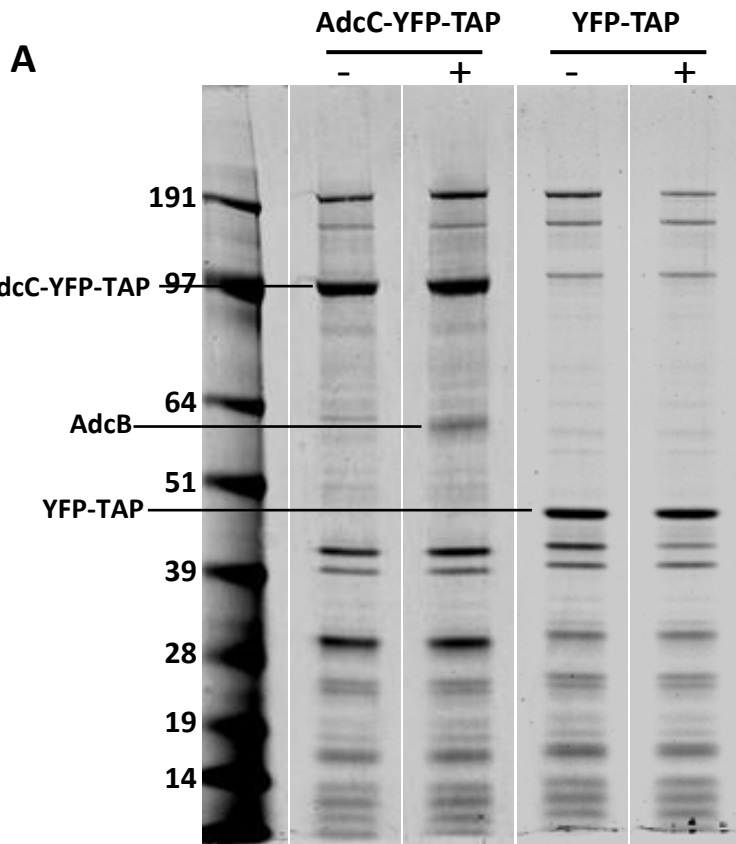
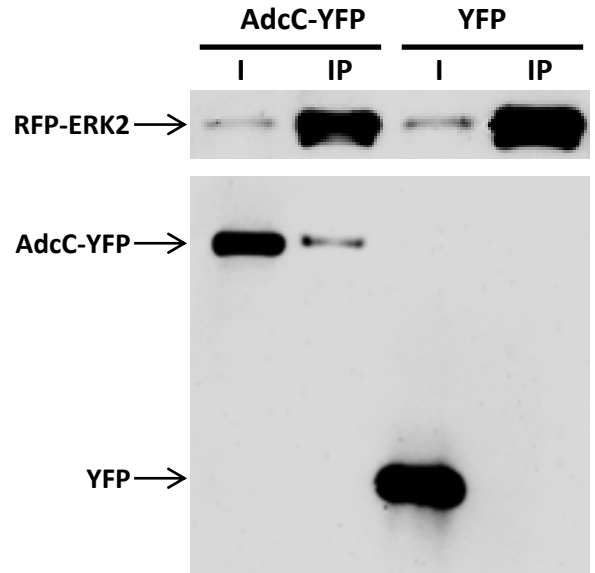






A*adcB*/AdcB-YFP**B**



**C****B**

MW (k Da)	Gene ID	Gene Name	Gene product	No. of Unique Peptides			
				AdcC+cAMP	AdcC w/o cAMP	control+cAMP	control w/o cAMP
74.2	DDB_G0271022	adcC	Arrestin Domain-Containing protein	38	33	0	0
70.1	DDB_G0274395	adcB	Arrestin Domain-Containing protein	25	20	0	0
64.5	DDB_G0292924	adcA	Arrestin Domain-Containing protein	2	0	0	0
193.5	DDB_G0277221	chcA	clathrin heavy chain	7	0	0	0
99.6	DDB_G0281957	ap1g1	clathrin-adaptor gamma chain	1	0	0	0
424.8	DDB_G0285063	DDB_G0285063	putative E3 ubiquitin-protein ligase	6	0	0	0
64.4	DDB_G0278981	DDB_G0278981	E3 ubiquitin-protein ligase	1	0	0	0
42.0	DDB_G0283903	erkB	ERK2	1	1	0	0

